Benha Journal of Applied Sciences (BJAS) **print: ISSN 2356–9751**
Vol. (9) Issue (1) (2024), (103-123) **online: ISSN 2356–976x**
http://bjas.bu.edu.eg

Finite Element Analysis of Strengthened R.C Flat Slab Edge Column Connections subjected to Punching Shear

M. I. Omar [1], K. M. Elsayed [2] and G. I. Khaleel [3]

[1]Department of Civil Engineering, Benha Faculty of Engineering, Benha university, Benha, Egypt,
, Assistant lecturer Mostafa.omar@bhit.bu.edu.eg,
[2] Department of Civil Engineering, Benha Faculty of Engineering, Benha university - Professor of Properties and Strength of Materials.
[3] Department of Civil Engineering, Benha Faculty of Engineering, Benha university - Emeritus Professor of RC Structures.
Mostafa.omar@bhit.bu.edu.eg.

Abstract

Nowadays, reinforced concrete (RC) flat slab system is used in many projects, even though, possibility of common problems in the slab-column connection that can cause a punching shear failure. Furthermore, an unbalanced moment may occur especially in the case of edge columns, which cannot be avoided. Therefore, in this study, the moment values have been considered. The most common procedure used to avoid this problem is punching shear strengthening, as it can increase joint strength capacity. 3D nonlinear finite element model (FEM) software, ABAQUS, based on the concrete damaged plasticity model, was used in order to investigate the punching shear reinforcement efficiency and study the connection behavior. The material model definition is necessary in finite element modeling to be appropriated [1]. A simulation of the FEM was compared with experimentally fifteen tested specimens, as investigated in [2]. Types, shapes, and cross-sectional area of the strengthening materials, as well as, the load eccentricity value, were the main studied parameters. The punching shear load-deflection relationship, the ultimate load, and the pattern of failure were demonstrated by this simulation. The numerical and experimental behavior comparison results obtained a reasonable response.

Keywords: Punching shear strengthening, edge column-flat slab connections, finite element model, concrete damaged plasticity and ABAQUS.

1. Introduction

Reinforced concrete flat slabs are the popular structural solution for several issues today because of their many architectural benefits, despite, the possibility of their sudden collapse at the critical section between the column's boundary and the slab due to punching shear failure. Shear reinforcement contributed significantly to avoiding this phenomenon, as it increases the connection strength capacity [3]. This phenomenon is getting worse in the case of the edge-column connection due to the asymmetry of the spans or loads, which could generate a developing moment [4]. Fig (1) shows how slab edge column connections are affected due to moment action in addition to vertical shear force [5]. The developed moment effected on the slabs strength can be considered by Ketut Sudarsana, which is approximately 67% of the pure punching shear connection strength. Strengthening is required when an already existing building needs its strength to be enhanced [6]. The pattern of failure on the slab round the column is following up the unbalance moment direction [7]. To date, several experimental tests have been conducted to investigate the behavior of flat slabs vulnerable to punching shear stresses. Now, after the need for more practical experiments, which demand resources like more funds, a long time, physical exertion, and the appropriate equipped space, finite element analysis (FEA) has become essential [8]. FEA can complement experimental test studies and provide insight into punching shear behavior; however, it's needed to be calibrated via a subset of experimental data [1]. Paiva, Lima Neto, Ferreira, Teixeira, and Oliveira [9] developed a large database by experimentally testing 131 slab rectangular column connections. Five tested slabs were examined by Aikaterini S. Genikomsou and Maria Anna Polak, two edge column specimens were subjected to horizontal and static loads, one specimen was an interior slab-column connection that was subjected to static load and the other two were interior specimens that were subjected to static and reversed cyclic loads [10]. The comparison of the numerical and experimental results showed that the calibration of these models accurately predicted the appropriate response. Aikaterini also, tested four interior slab column specimens subjected to vertical load, the main parameter was the shear reinforcement amount, and the results were compared with a FEA which indicated a great convergence [11]. G. I. Khaleel and Mohamed H. Makhlouf experimentally tested six strengthened specimens subjected to eccentric punching shear load which gained about 60% capacity enhancement then; they set a FEM to simulate these results which give a significant agreement [12]. Here, this investigation shows a calibrated FEM set for simulation of punching shear-strengthened fifteen experimentally tested specimens in the Reinforced Concrete Laboratory, at Benha Faculty of Engineering by G. I. Khaleel, K. M. Elsayed and M. I. Omar [1], which studied the effect of shear reinforcement using steel links, glass

fiber reinforced polymer (GFRP), and carbon fiber reinforced polymer (CFRP) as manually prepared stirrups as shown in Fig (2) The fifteen tested specimens were divided into five groups as full details are explained in [1]. The experimentally studied parameters were the eccentric load value, the strengthening material's type, and the strengthening element's shape and amount. The concrete damage plasticity model in the FEM software ABAQUS is used for modeling.

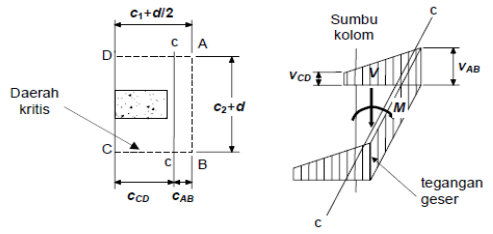

Fig. (1) Eccentric shear stress model under vertical load V and unbalanced bending moment M [5].

2. TEST SPECIMENS

The considered FEM in this investigation has been developed based on the previously indicated experimental investigation in [1]. This study contained fifteen tested specimens having the same geometrical dimensions, structural details, material properties and flexural reinforcement. All the specimen's dimensions were 900*900*130 mm for the slab, with a cross sectional area of edge-columns of 150*150 mm and extended by 300 mm length under the slab lower face and 50 mm above the upper slab top face. A 150 mm clear length column leg cantilever was projected at the lower column extension with the same column cross-sectional area, for providing a suitable space for load eccentricity. Fig (2) shows the dimensions, reinforcement, supports, and points of loading for the fifteen specimens. According to the study [1] parameters, the fifteen specimens have been divided into five groups as shown in Table (1). The first one, as named group one, was a three control specimens without shear reinforcement loaded by variant eccentricity values (0, e, and 2e). The other four groups were strengthened by variant shear reinforcement systems (CFRP, GFRP and steel links), two groups –group no. two and group no. four- were strengthened using one strengthening row, while the last two groups -group no. three and group no. five-were strengthened by two strengthening rows. Also, groups no. two and no. three were loaded by eccentric loads with a value (e) of eccentricity, while groups no. four and no. five were loaded by eccentric loads with a value (2e) of eccentricity. Flexural reinforcement was considered as, flexural failure never occurred before failure due to punching shear. Specimens flexural reinforcement, dimensions, supports and strengthening systems details are shown in Fig (2:4).

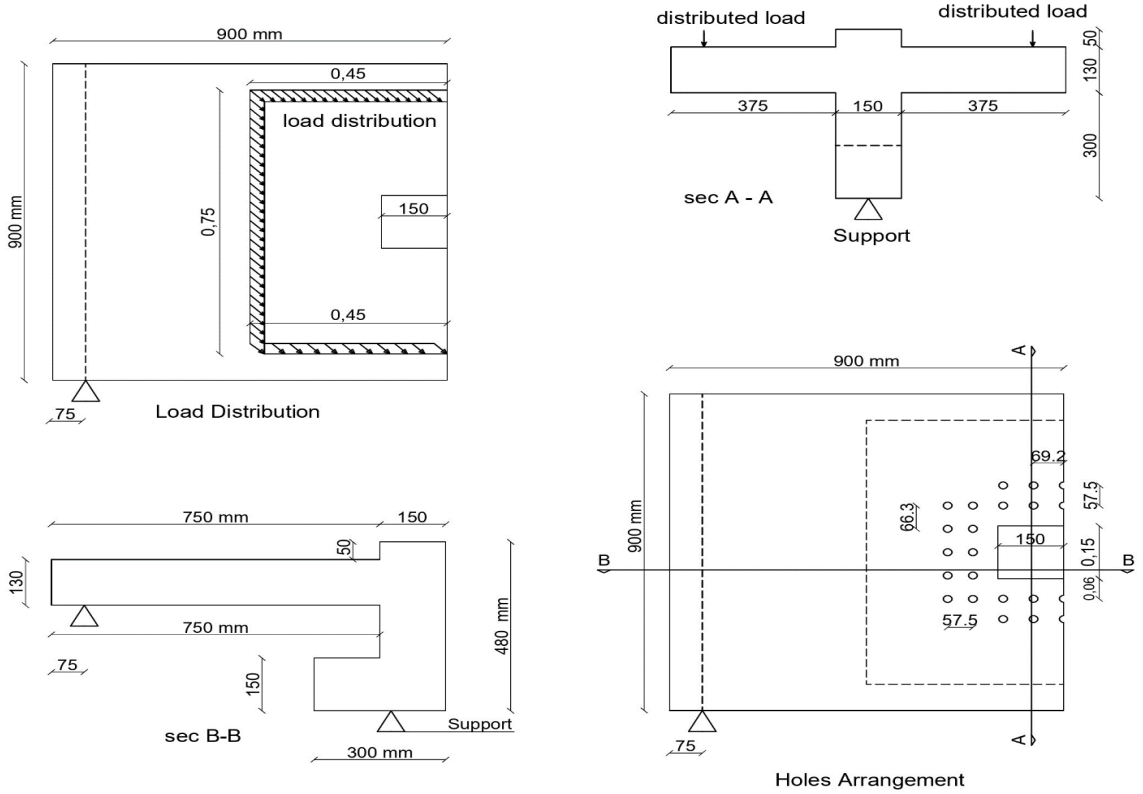

Fig. (2) The specimens' dimensions and supports [1].

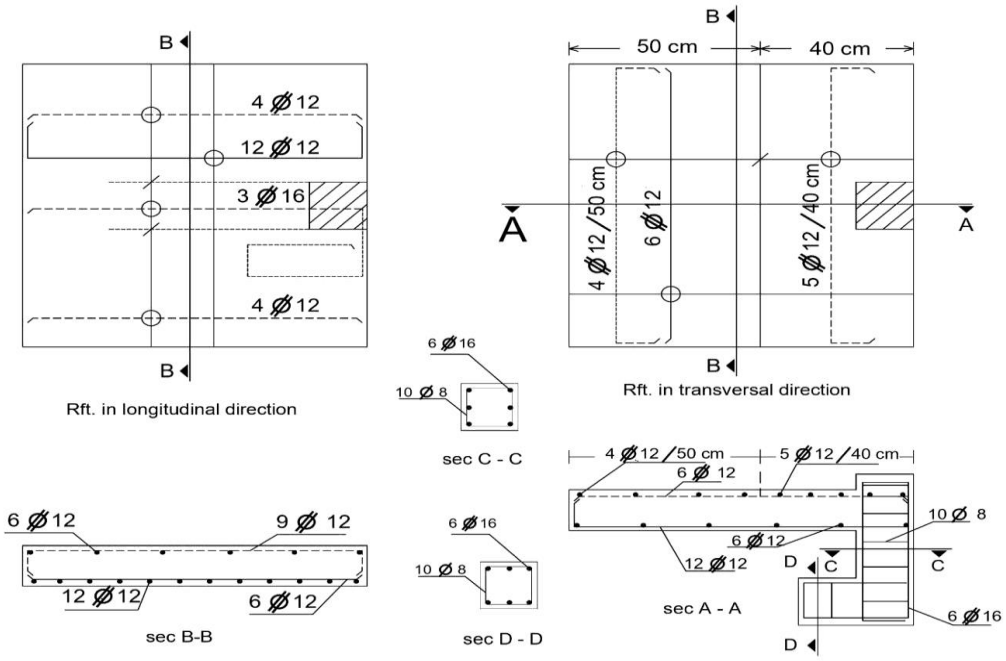

Fig. (3) The specimen's reinforcement [1]

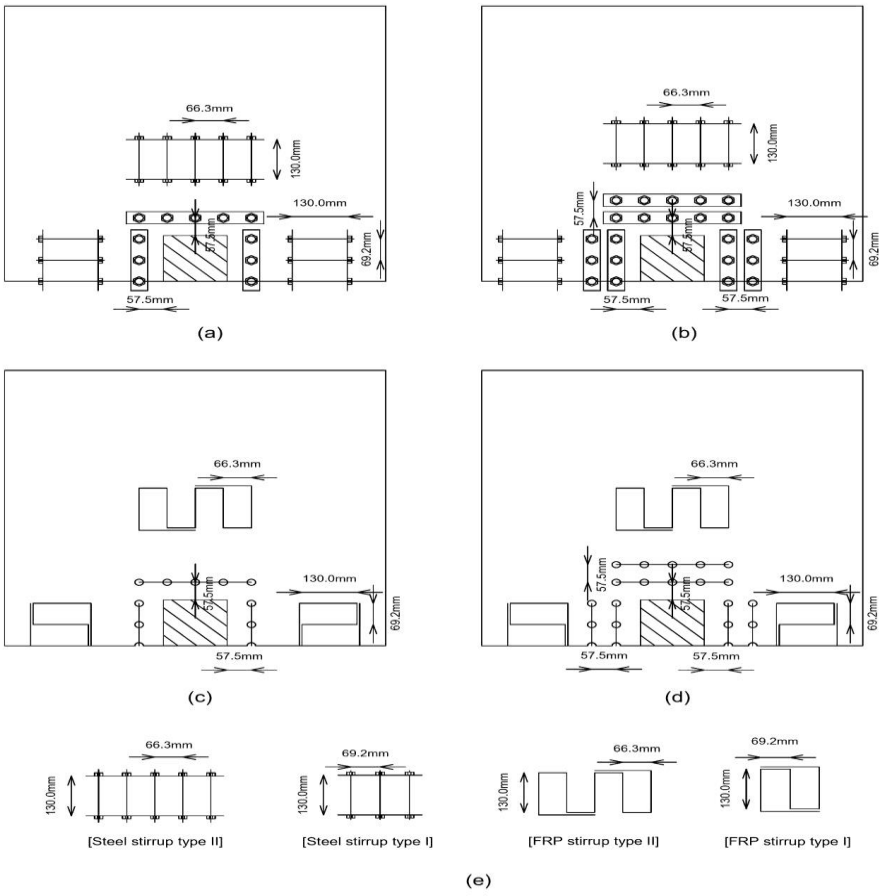

Fig. (4) Details of strengthening systems; Using one row of steel links (a), steel two rows (b), FRP one row of stirrups (c), FRP two rows stirrups (d) Details of stirrups types (e) [1].

Table (1): Specimens details [1].

Group	Specimen code	Specimen case	Rows number	Eccentricity value (mm)	Strengthening material
	C	control	----------	0	----------
No. 1	C-1e	control	----------	50	----------
	C-2e	control	----------	100	----------
	SC1-1e	Strengthened	1	50	CFRP stirrups
No. 2	SG1-1e	Strengthened	1	50	GFRP stirrups
	SS1-1e	Strengthened	1	50	Steel Links
	SC2-1e	Strengthened	2	50	CFRP stirrups
No. 3	SG2-1e	Strengthened	2	50	GFRP stirrups
	SS2-1e	Strengthened	2	50	Steel Links
	SC1-2e	Strengthened	1	100	CFRP stirrups
No. 4	SG1-2e	Strengthened	1	100	GFRP stirrups
	SS1-2e	Strengthened	1	100	Steel Links
	SC2-2e	Strengthened	2	100	CFRP stirrups
No. 5	SG2-2e	Strengthened	2	100	GFRP stirrups
	SS2-2e	Strengthened	2	100	Steel Links

3. FINITE ELEMENT SIMULATION

3.1. Methodology

These days, FEA is the most recent technique for investigating the structural behavior of different elements. Many software programs have been developed to use FEA methodologies to numerically study structural behavior , especially punching shear behavior. In this study, ABAQUS/CAE was used, which is a multi-purpose analysis product that uses standard static FE modes. It can be used to simulate raising loads as nature. Numerical simulation in Abaqus is usually done in many steps to finish the model solution [13], Fig. (5) Shows these steps.

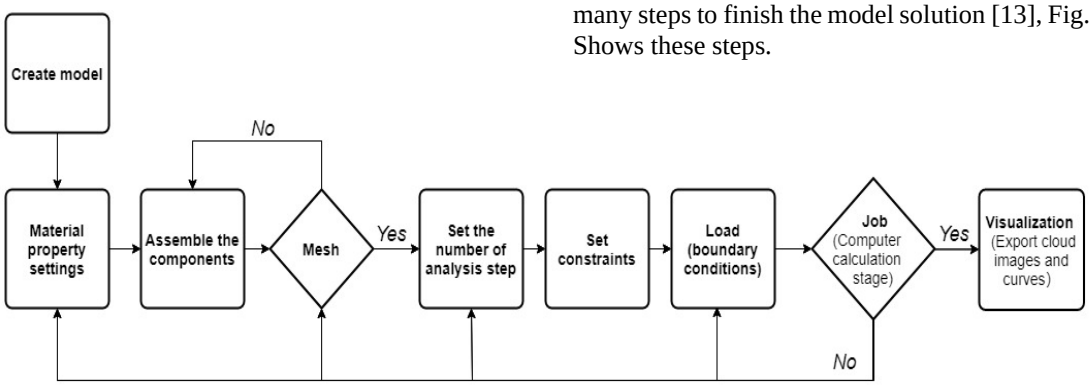

Fig. (5) Simulation flow chart [13].

3.2. Elements Description

Three major types of elements are used to create a 3D FEM; solid element for the concrete slab, truss (wire) element for reinforcement bars and steel stirrups and shell element for strengthening FRP stirrups system.

3.2.1. Solid Element

As seen in Fig (6 & 7), the concrete slab column connection and the steel plates used with strengthe-ning steel links were created using the sold brick element (C3D8R), where C refers to the solid element, 3D is three-dimensional, 8 means the number of nodes in this unit, and R refers to this unit as a reduced integrated unit, while this element contains three transitional degree of freedom for each node [4]. This element was selected as it has the ability to specify the concrete slab's boundary as well as the contact surfaces required for load applying FRP stirrup strengthening, and boundary conditions.

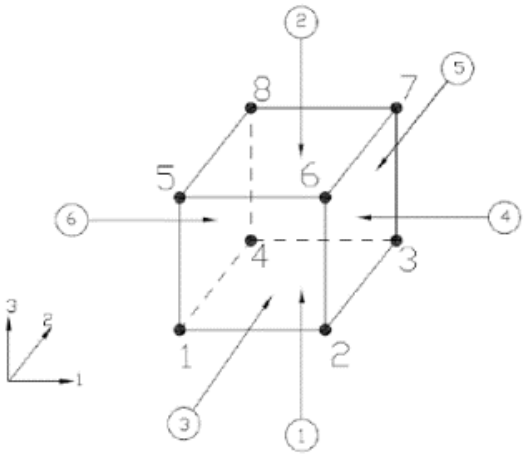

Fig. (6) 3-Dimensional solid (Brick) element.

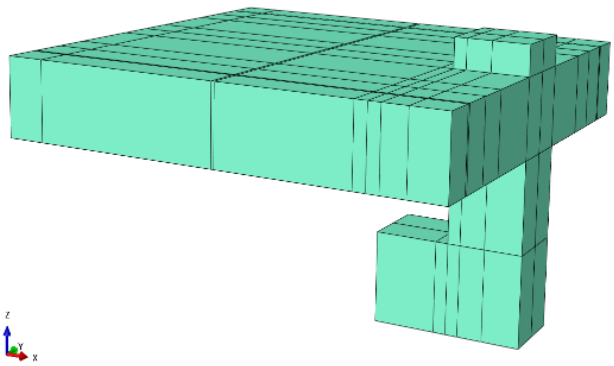

Fig. (7) Concrete part.

3.2.2. Truss Element

This type of element is a 2-node linear element (T3D2), it can resist axial force only, that is, can't carry bending yet as recommended by Kenea and Megarsa [15], and Attia et al. [16], there for, it is appropriate with flexural reinforcement and strengthening steel links as shown in Fig (8).

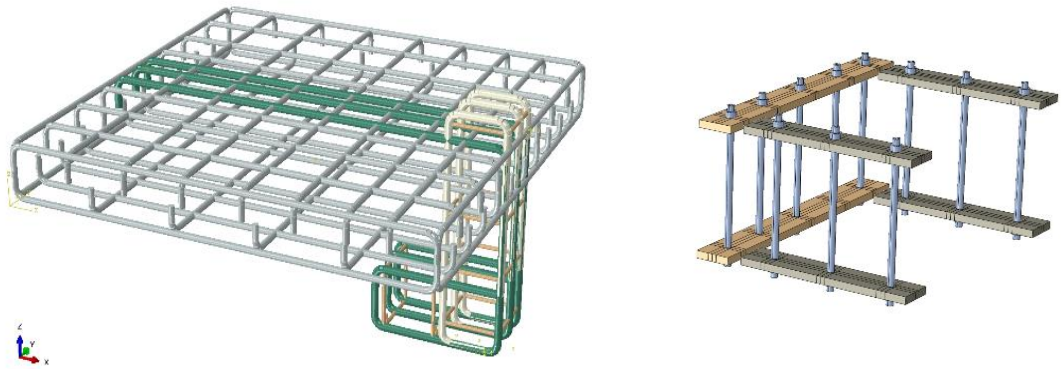

Fig. (8): Flexural reinforcement and steel links modeling as truss element steel plates modeling as solid element.

3.2.3. Shell Element

Conventional shell element type was used for modeling FRP strengthening stirrups as shown in Fig. (9) Conventional shell elements include thin and thick shell elements such as (S4R5) and (S4R6), respectively. The thin shell elements have five degrees of freedom (DOF) per node, while the thick shell elements have six DOF per node [17]. Shell thin element S4R6 was used for modeling FRP Stirrups.

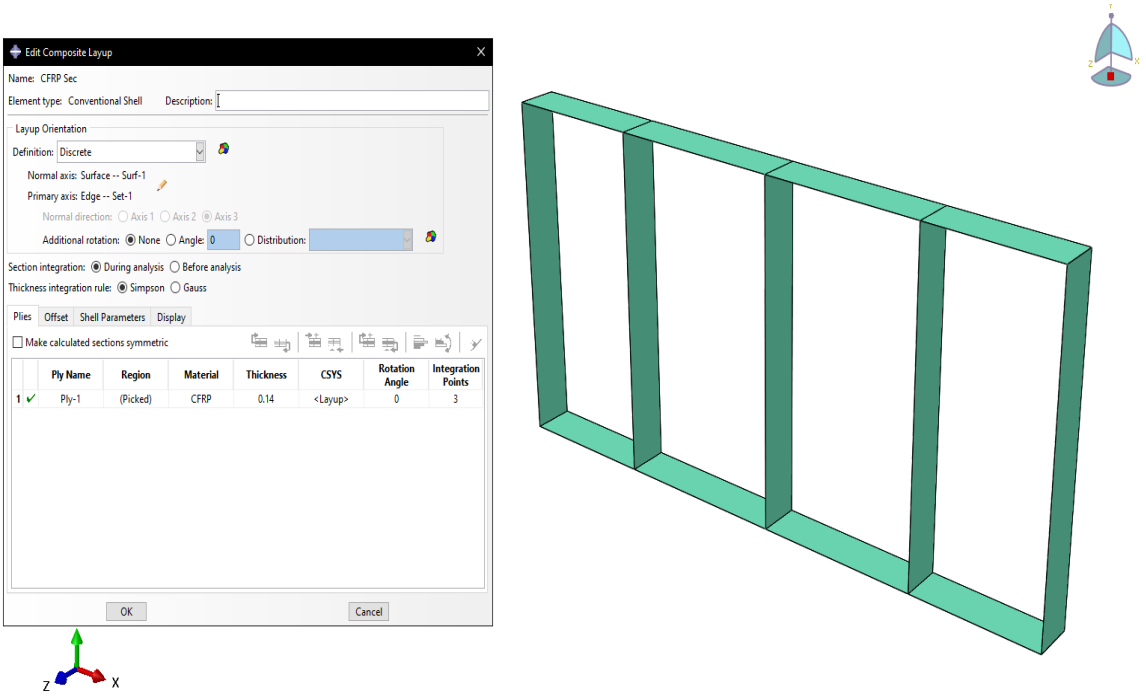

Fig. (9) FRP strenthgning stirrups modeling as shell elements.

3.3. Material Modeling

To create FEM, three different models of materials from ABAQUS [18] are used. The first one is the concrete-damaged plasticity model (CDP) that was used for concrete modeling, the second one used to model steel reinforcement is the elastic-plastic model, and the third one is the elastic model which used for FRP strengthening stirrups

3.3.1. Concrete Damage Plasticity Model

Concrete damage plasticity model (CDP) is used for modeling concrete because of its ability of simulating concrete's plastic properties and consider the concrete behavior in compression and tension [17] as shown in Fig. (10). While in this model, compressive crushing and tensile cracking are the main failure modes [19].

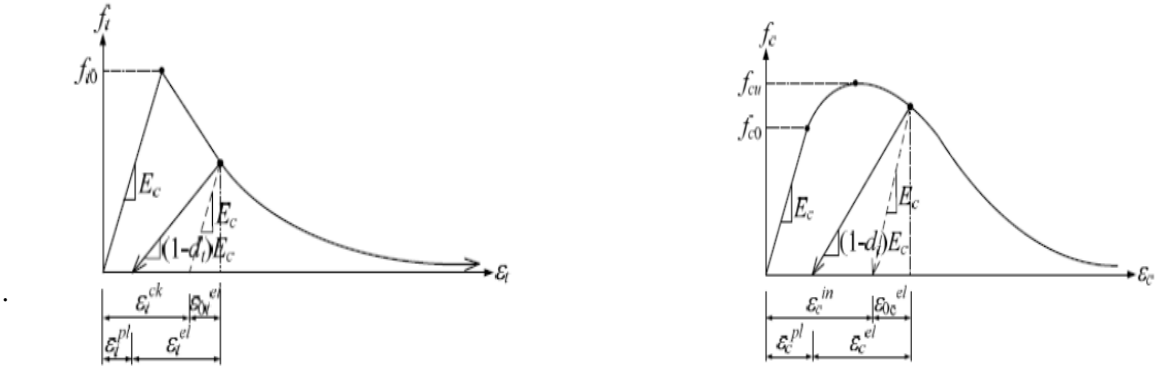

(a) Tensile Behavior Associated with Tension Stiffening

(b) Compression behavior associated with compression hardening.

Fig. (10) Concrete damaged plasticity model [17].

Table (2): Elastic properties of concrete.

Concrete Parameters	
Density, kg/m^3	2200
Modulus of elasticity (Ec)	20200 MPa
Poisson's ratio (υ)	0.20

Table (3): Concrete damaged plasticity parameters [10].

Concrete Parameters	
Dilation angle	39
Eccentricity	0.12
Fb_o/fc_o	1.36
K	0.67
Viscosity parameter	0.000001
Compressive ultimate stress	25.0 MPa
Tensile ultimate stress	2.50 MPa

3.3.2. Elastic-Plastic Model

The steel reinforcement bars and steel links behavior were represented in ABAQUS using elastic-plastic model. First, steel behaves as a linear elastic state as long the steel strain is of a lower value, its defined by the Young's or elastic modulus, when its gains a higher strain value, its begin to be nonlinear, which is defined by plasticity state. The limit of steel plastic behavior is described by the yield point, if the applied load is removed, the steel will fully recover from any elastic strains done by the deformation that occurred before it reached the yield point. On the other hand, constant (plastic) deformation starts to happen when the steel's stress goes above the yield stress. Fig. (11) shows the stress-strain curve for elastic-plastic materials.

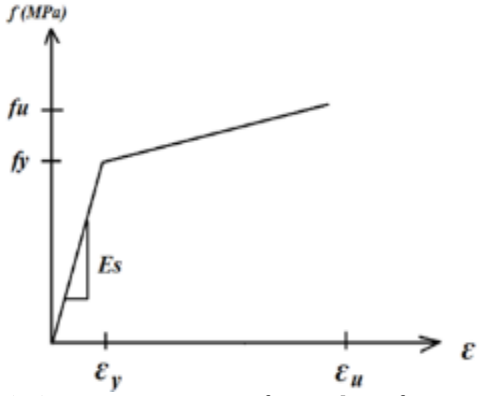

Fig. (11) Stress-strain curve for steel reinforcement in FEA.

3.3.3. Elastic Model

FRP stirrups act approximately linear elastic state behavior when the stress given by the elastic modulus stays constant at low strain values. Therefore, it was represented using the elastic material model in ABAQUS. Fig (13) illustrates the stress-strain curve for elastic materials.

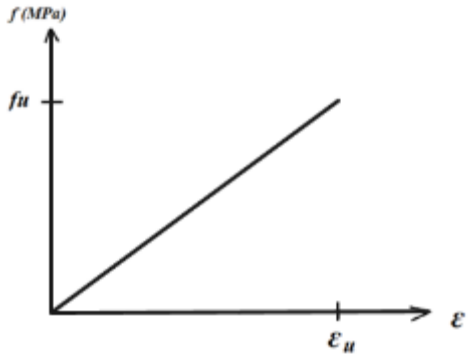

Fig. (12) The stress-strain curve for elastic materials.

3.4. Finite Element Results and Discussion

Through comparison of the numerical and experimental results, the finite element model created in this study will be validated.

3.4.1. Ultimate Load Comparison

As the ultimate load comparison between FEM and experimental tests has been done, a little deference in ultimate load values has observed, which shows that the FEM simulation has a high accuracy as its give a close result to the experiments. The maximum difference between FEM and Experimental ultimate loads was 4.7% and the minimum difference was 0.6 %. Numerical simulations were performed under ideal input data. Fig (13) shows a comparison between experimental and FEM ultimate loads for all specimens. Also, Table (4) shows FEM and experimental ultimate loads.

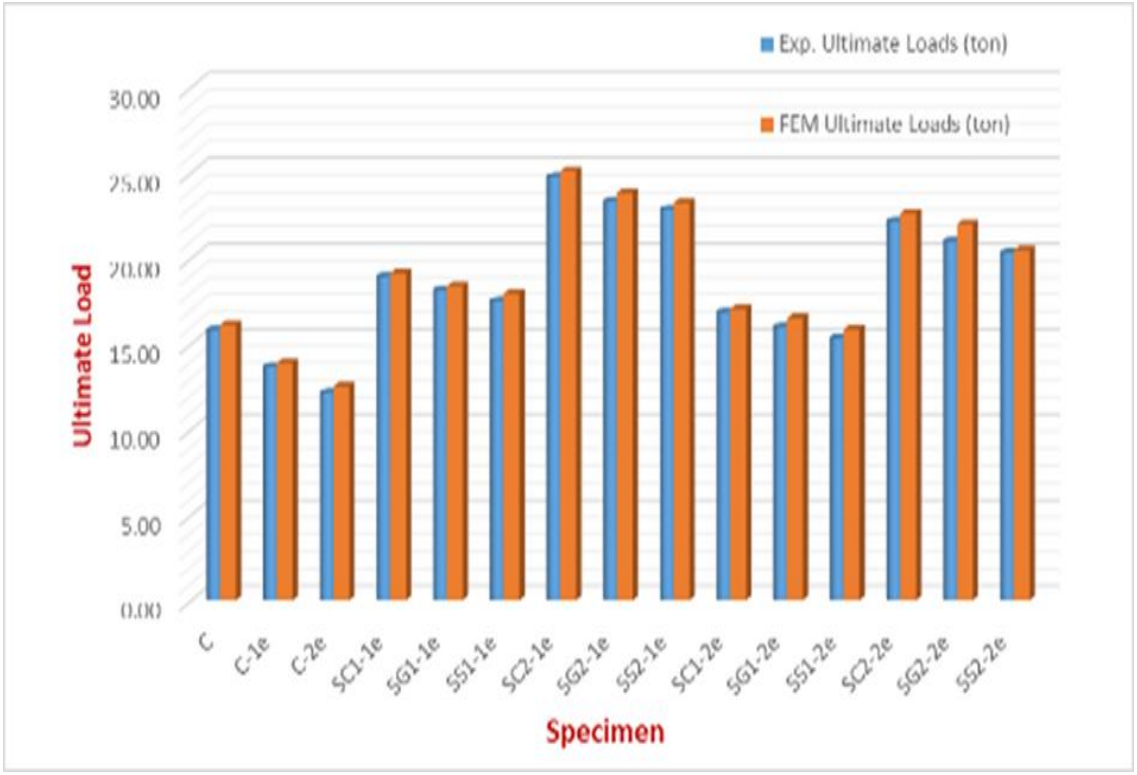

Fig. (13) Comparison between experimental and FEM results of ultimate loads for all specimens.

Table (4): Comparison between experimental and numerical results.

Group	Specimen code	Ultimate Exp. Load (ton)	Ultimate FEM. load (ton)	FEM. Load / Exp. Load
No. 1	C	15.8	16.01	1.013
	C-1e	13.64	13.87	1.017
	C-2e	12.13	12.49	1.030
No. 2	SC1-1e	18.92	19.11	1.010
	SG1-1e	18.12	18.36	1.013
	SS1-1e	17.18	17.92	1.043
No. 3	SC2-1e	24.75	25.07	1.013
	SG2-1e	23.3	23.82	1.022
	SS2-1e	22.63	23.22	1.026
No. 4	SC1-2e	16.83	17.02	1.011
	SG1-2e	15.97	16.48	1.032
	SS1-2e	15.2	15.83	1.041
No. 5	SC2-2e	22.15	22.63	1.022
	SG2-2e	20.98	21.97	1.047
	SS2-2e	20.32	20.45	1.006

3.4.2. Load-deflection Comparisons

The specimen's midpoint displacement is one of the important results that has been involved to predict specimen stiffness and strength. So that load-deflection at the midpoint relationship has detected experimentally and numerically.

As shown in Figs (14 to 28), load deflection curves for FEM and experimental tests are so close, it's illustrated that there is a little deviation of the compared results. Furthermore, the load-deflection curve comparisons showed good harmony between all experimental specimen results and the predicted FEM.

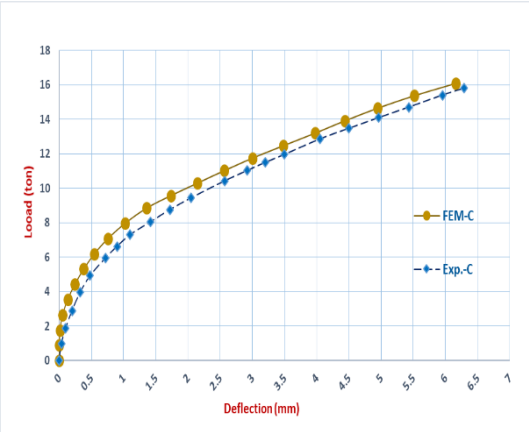

Fig (14) FEM and Exp. load-deflection relationship comparison for specimen (C).

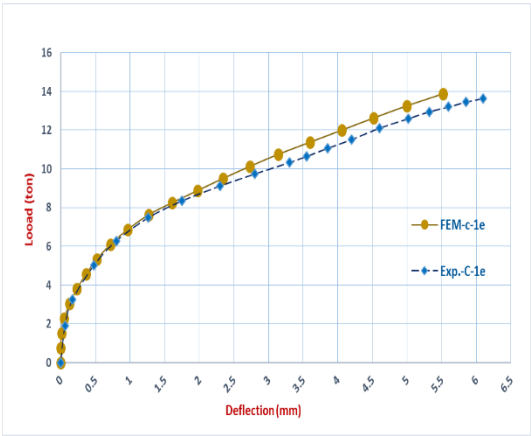

Fig (15) FEM and Exp. load-deflection relationship comparison for specimen (C-1e).

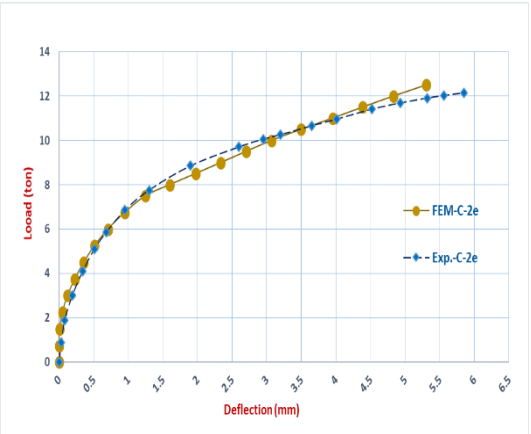

Fig (16) FEM and Exp. load-deflection relationship comparison for specimen (C-2e).

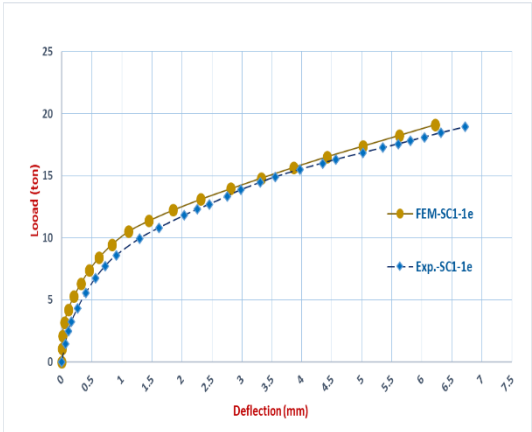

Fig (17) FEM and Exp. load-deflection relationship comparison for specimen (SC1-1e).

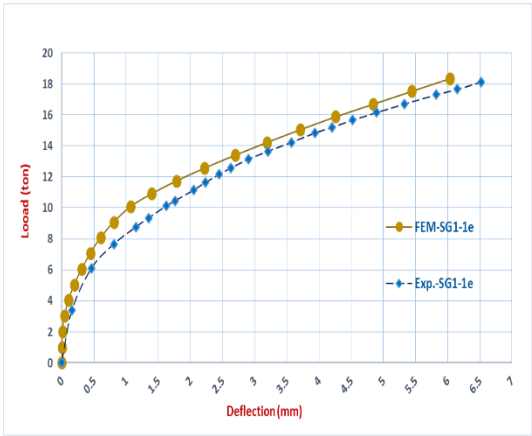

Fig (18) FEM and Exp. load-deflection relationship comparison for specimen (SG1-1e).

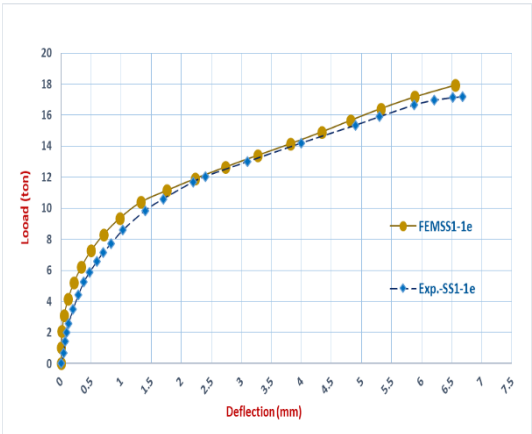

Fig (19) FEM and Exp. load-deflection relationship comparison for specimen (SS1-1e).

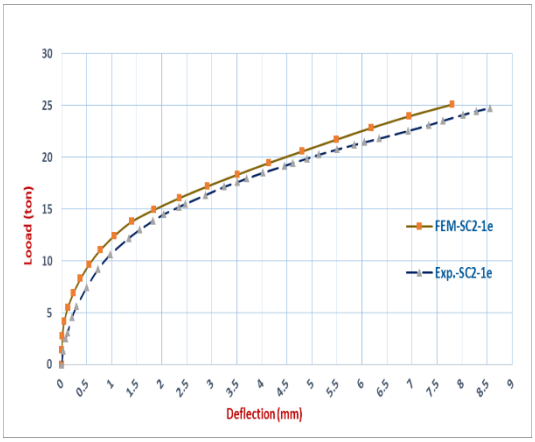

Fig (20) FEM and Exp. load-deflection relationship comparison for specimen (SC2-1e).

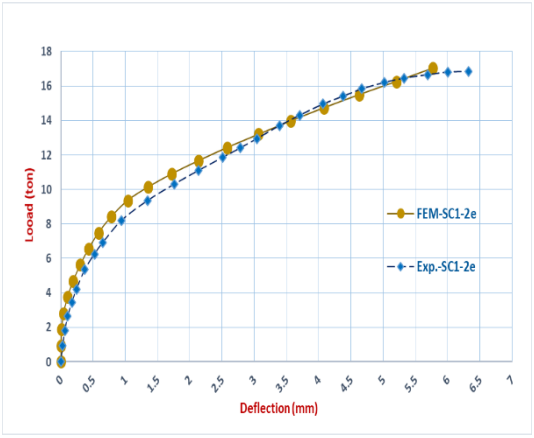

Fig (23) FEM and Exp. load-deflection relationship comparison for specimen (SC1-2e).

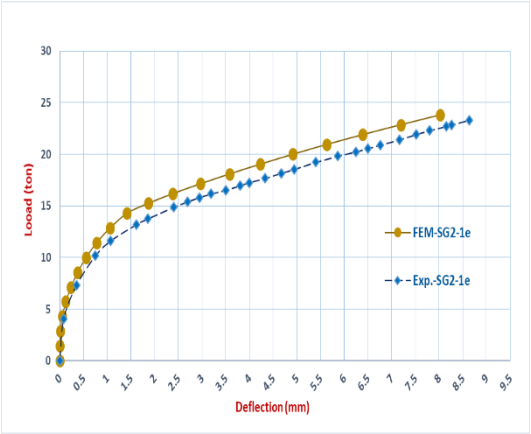

Fig (21) FEM and Exp. load-deflection relationship comparison for specimen (SG2-1e).

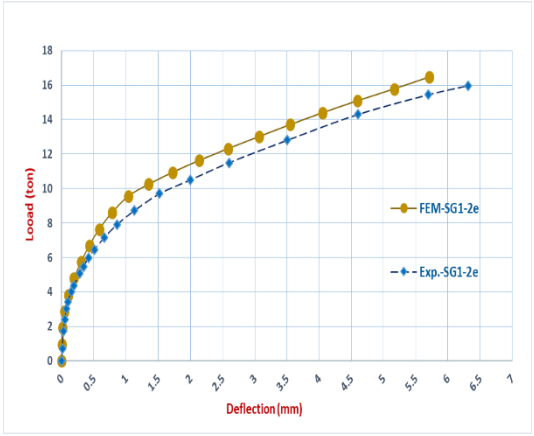

Fig. (24) FEM and Exp. load-deflection relationship comparison for specimen (SG1-2e).

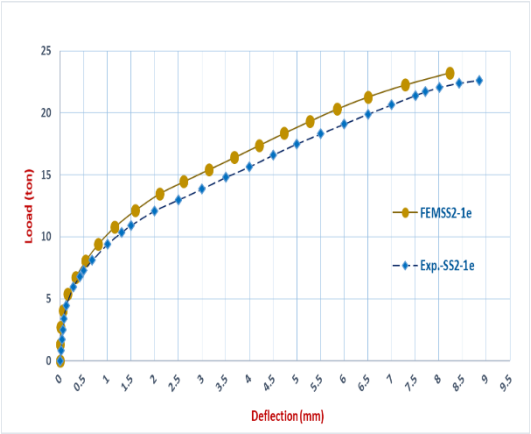

Fig (22) FEM and Exp. load-deflection relationship comparison for specimen (SS2-1e).

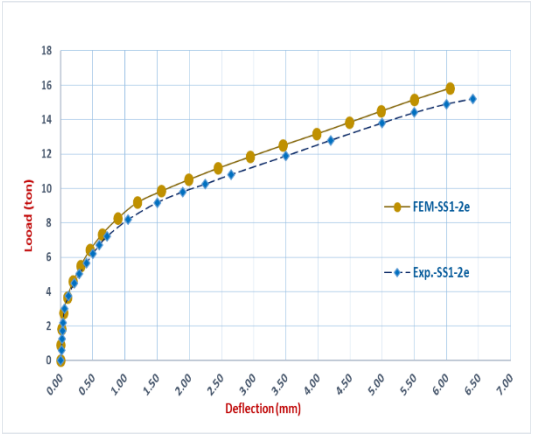

Fig. (25) FEM and Exp. load-deflection relationship comparison for specimen (SS1-2e).

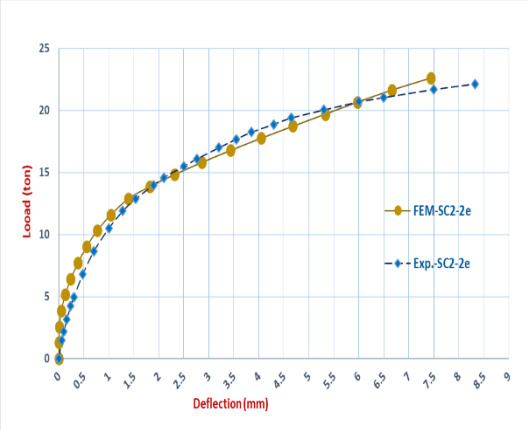

Fig. (26) FEM and Exp. load-deflection relationship comparison for specimen (SC2-2e).

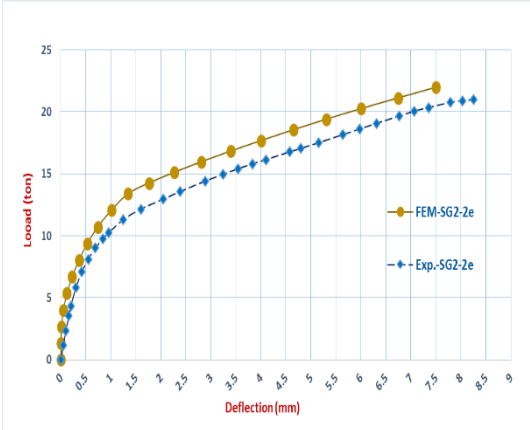

Fig. (27) FEM and Exp. load-deflection relationship comparison for specimen (SG2-2e).

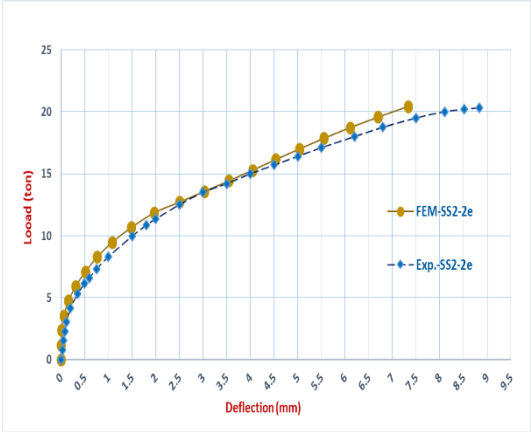

Fig. (28) FEM and Exp. load-deflection relationship comparison for specimen (SS2-2e).

3.4.3. Cracking Pattern Comparisons

Figs (29 to 43) show that the mode of failure for all FE specimens failed under punching shear. It was observed that it was quite similar to the experimental crack pattern. It's also confirms that FEM performed reasonably. For all the FE specimens, the cracks initiated near the edges of the columns on the underside of the slab penetrating the slab to form an incomplete inverted cone. It's also observed that the failure pattern was created entirely out of the strengthened zone.

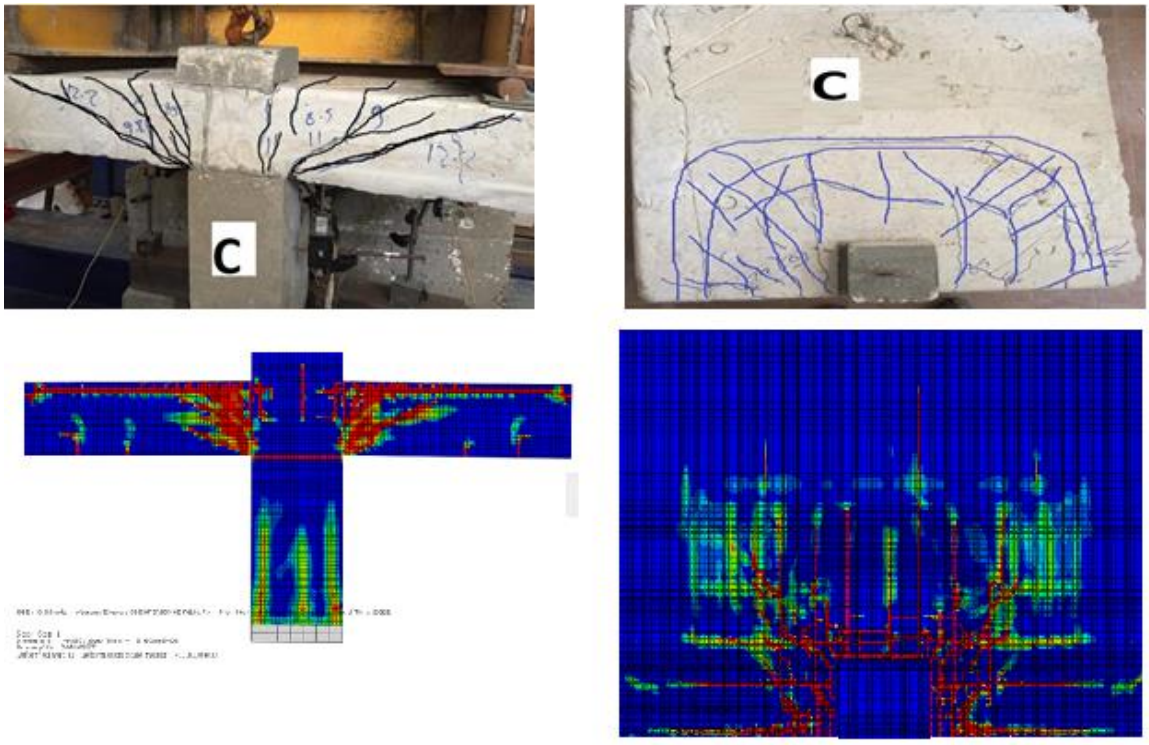

Fig. (29) FEM and Exp. pattern of failure comparison for specimen (C).

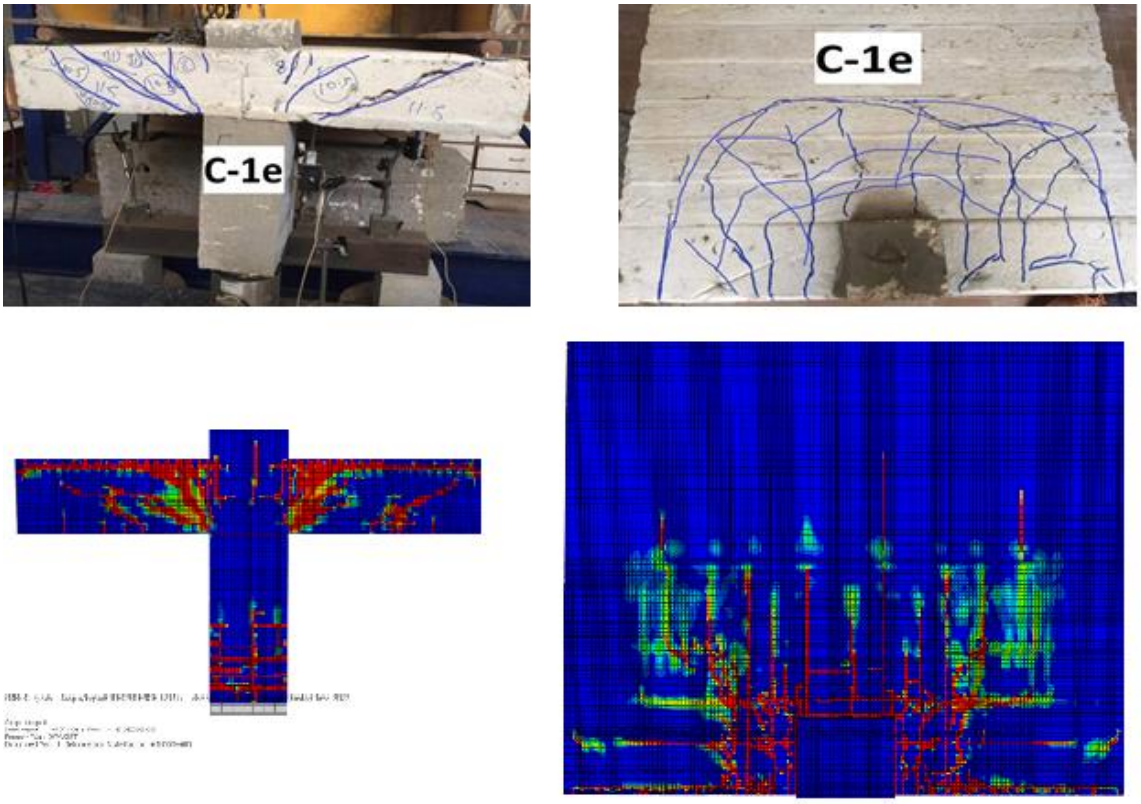

Fig. (30) FEM and Exp. pattern of failure comparison for specimen (C-1e).

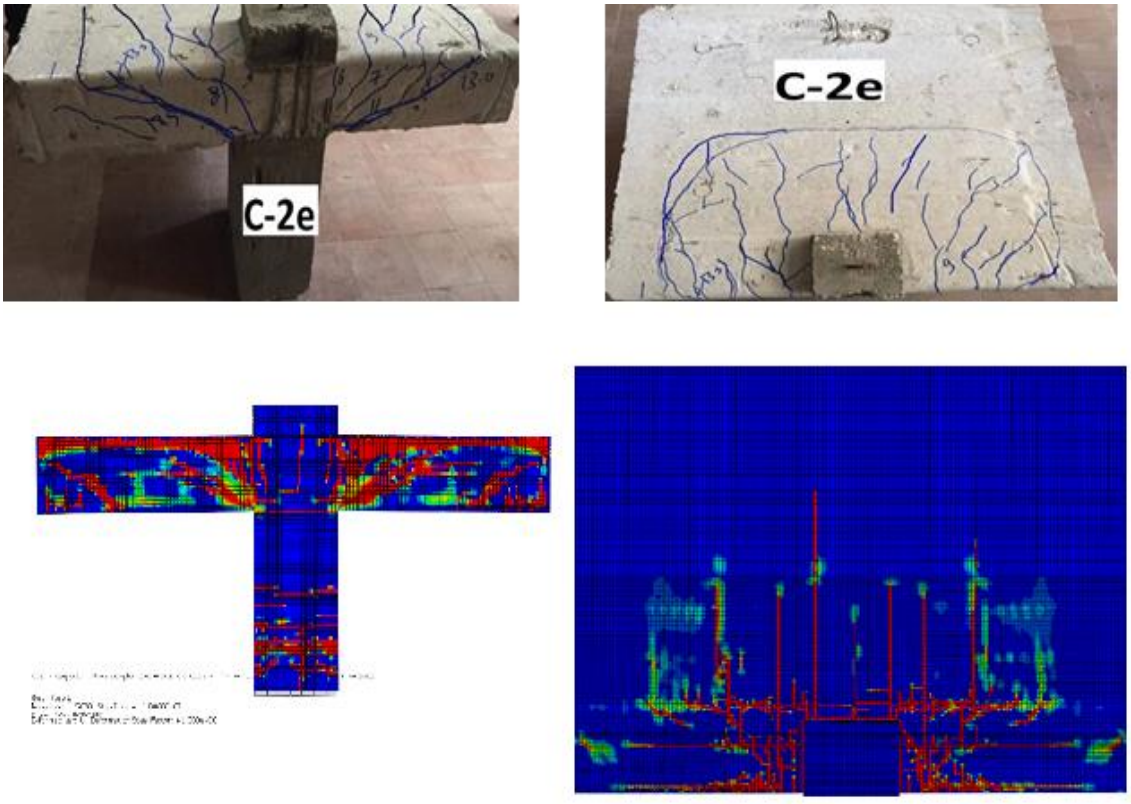

Fig. (31) FEM and Exp. pattern of failure comparison for specimen (C-2e).

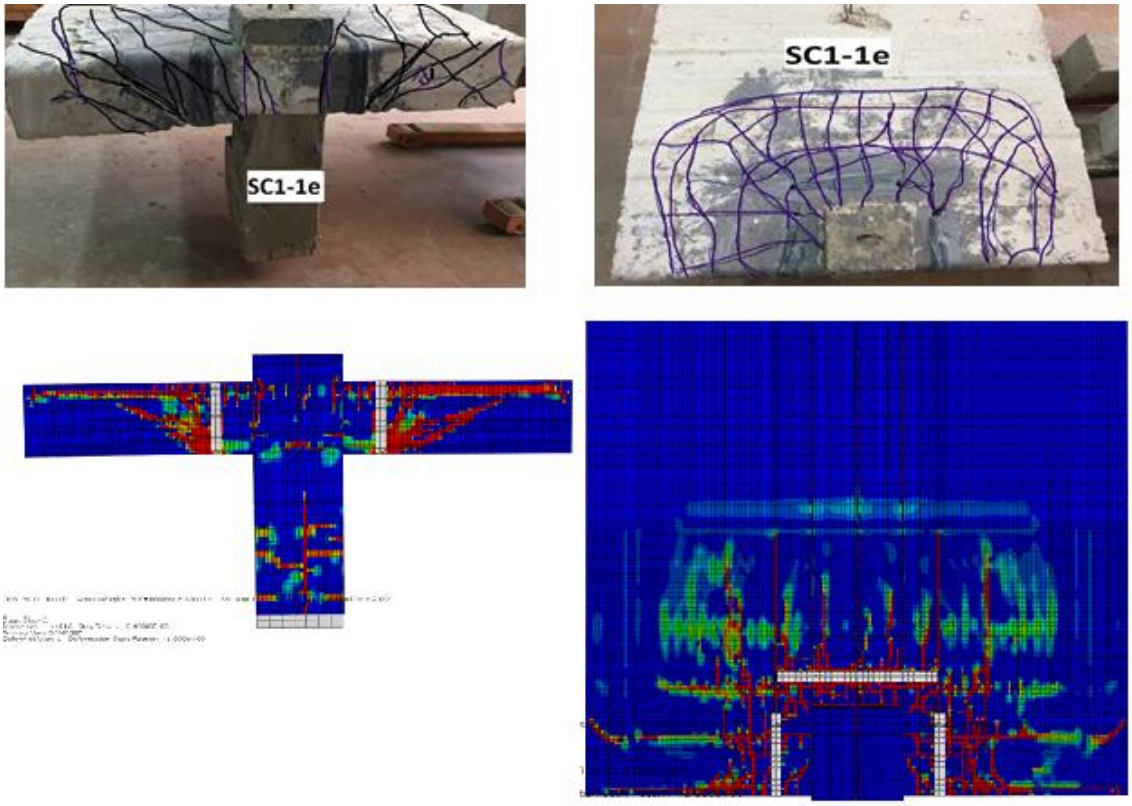

Fig. (32) FEM and Exp. pattern of failure comparison for specimen (SC1-1e).

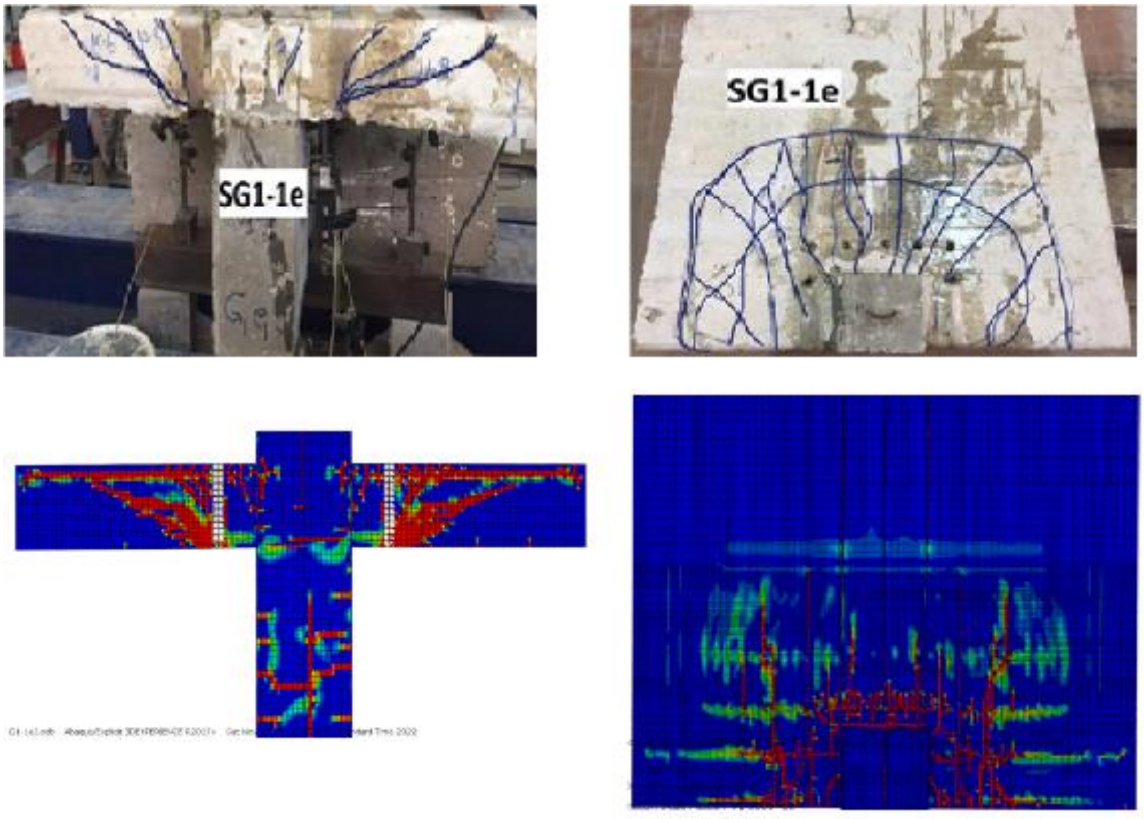

Fig. (33) FEM and Exp. pattern of failure comparison for specimen (SG1-1e).

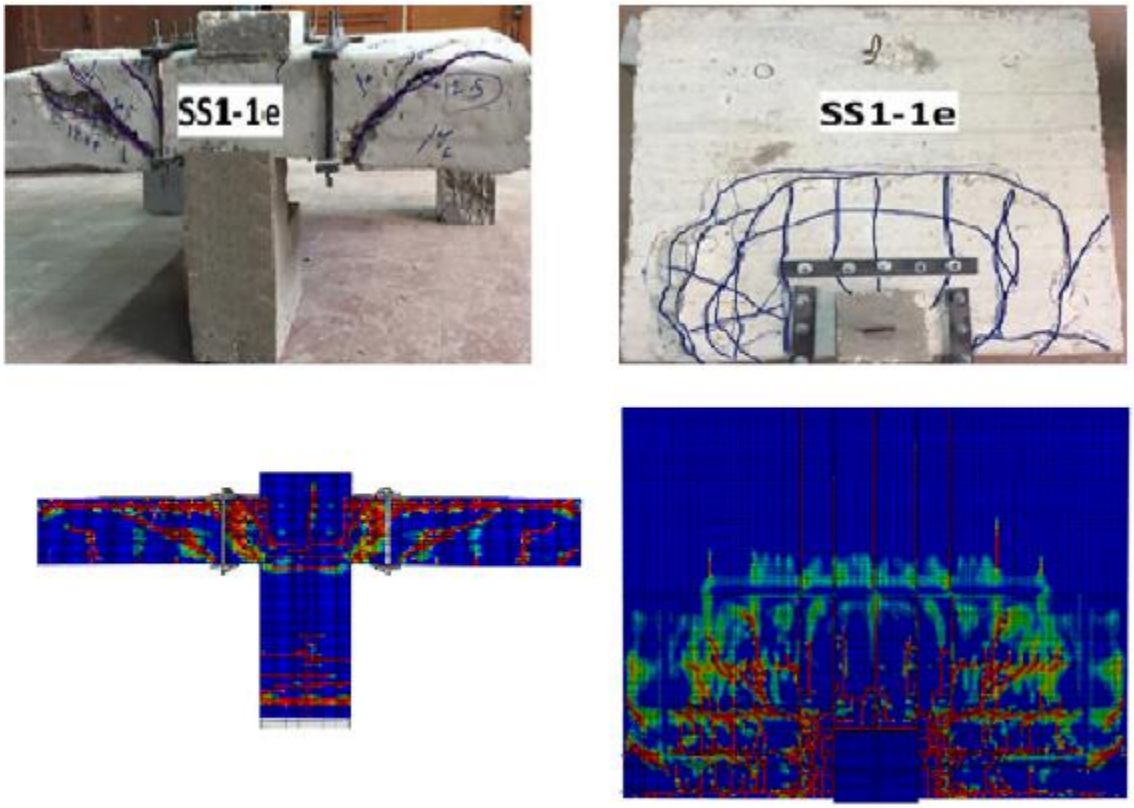

Fig. (34) FEM and Exp. pattern of failure comparison for specimen (SS1-1e).

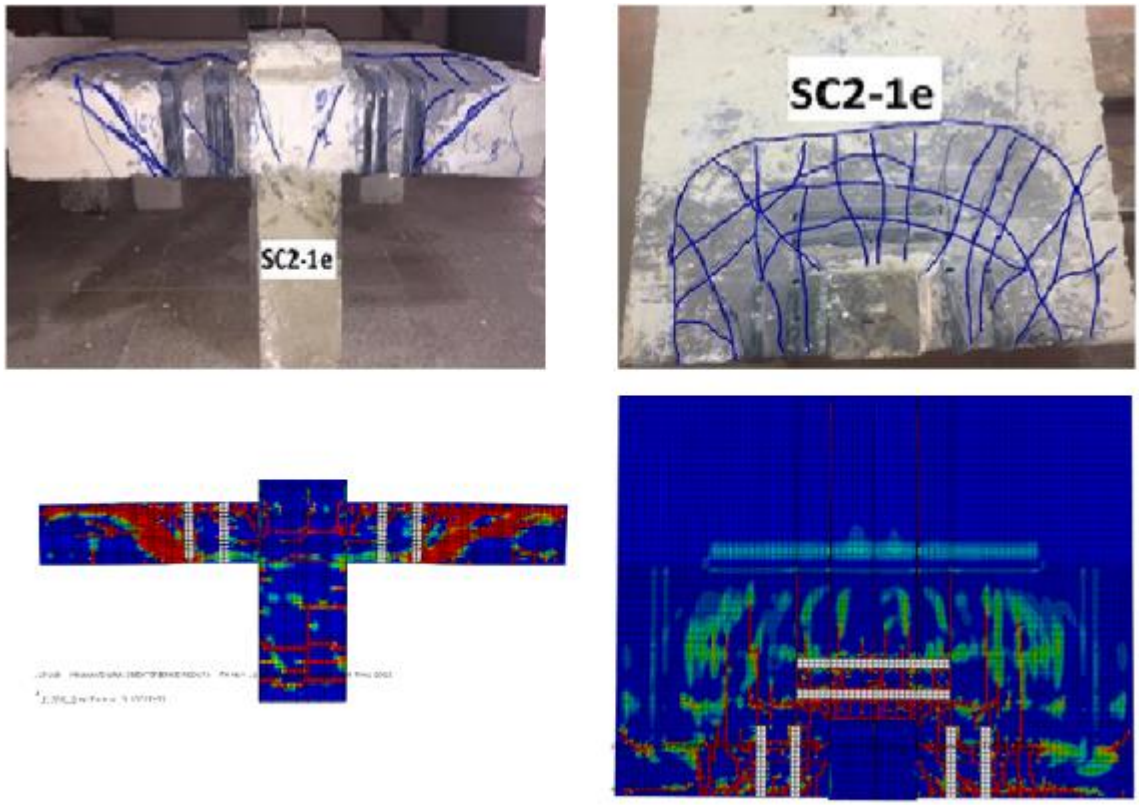

Fig. (35) FEM and Exp. pattern of failure comparison for specimen (SC2-1e).

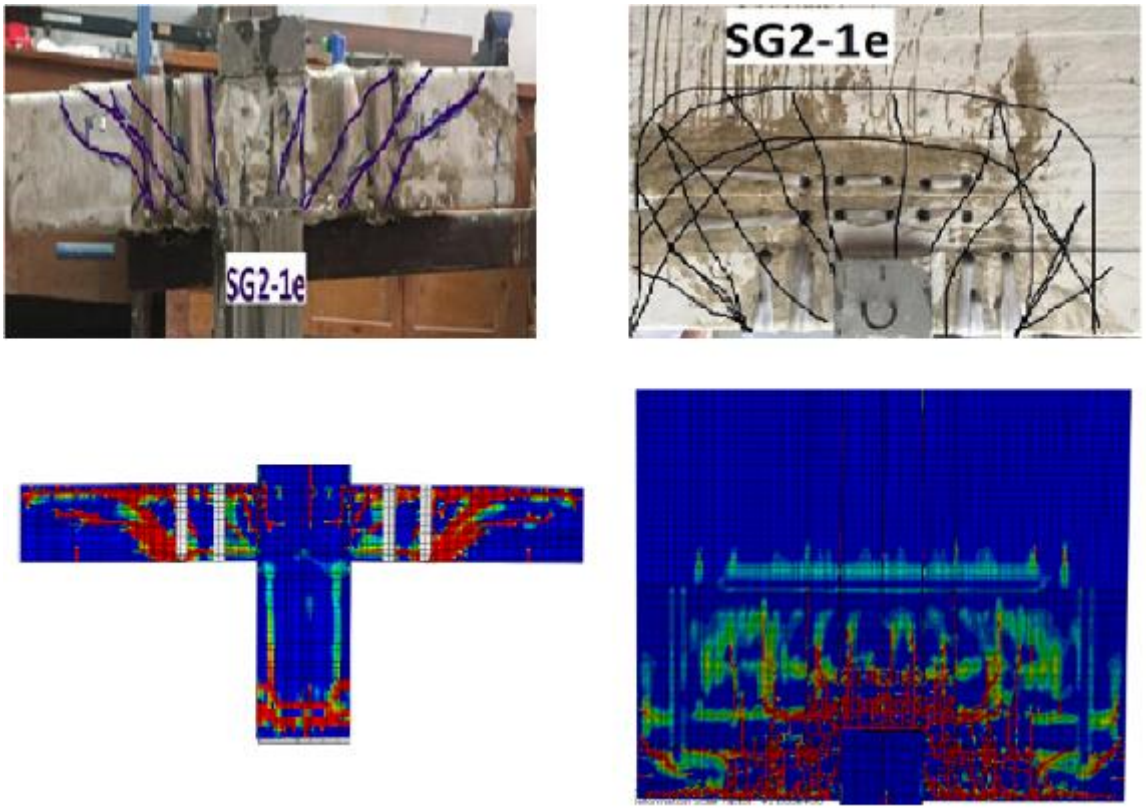

Fig. (36) FEM and Exp. pattern of failure comparison for specimen (SG2-1e).

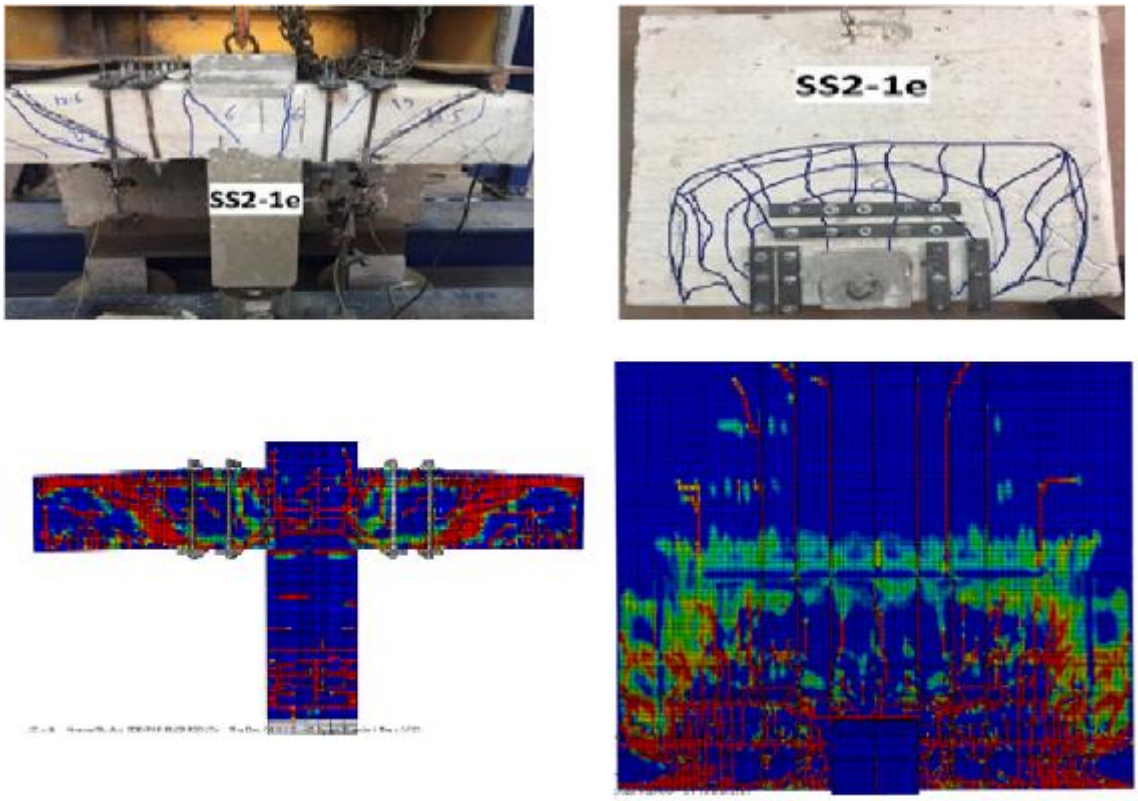

Fig. (37) FEM and Exp. pattern of failure comparison for specimen (SS2-1e).

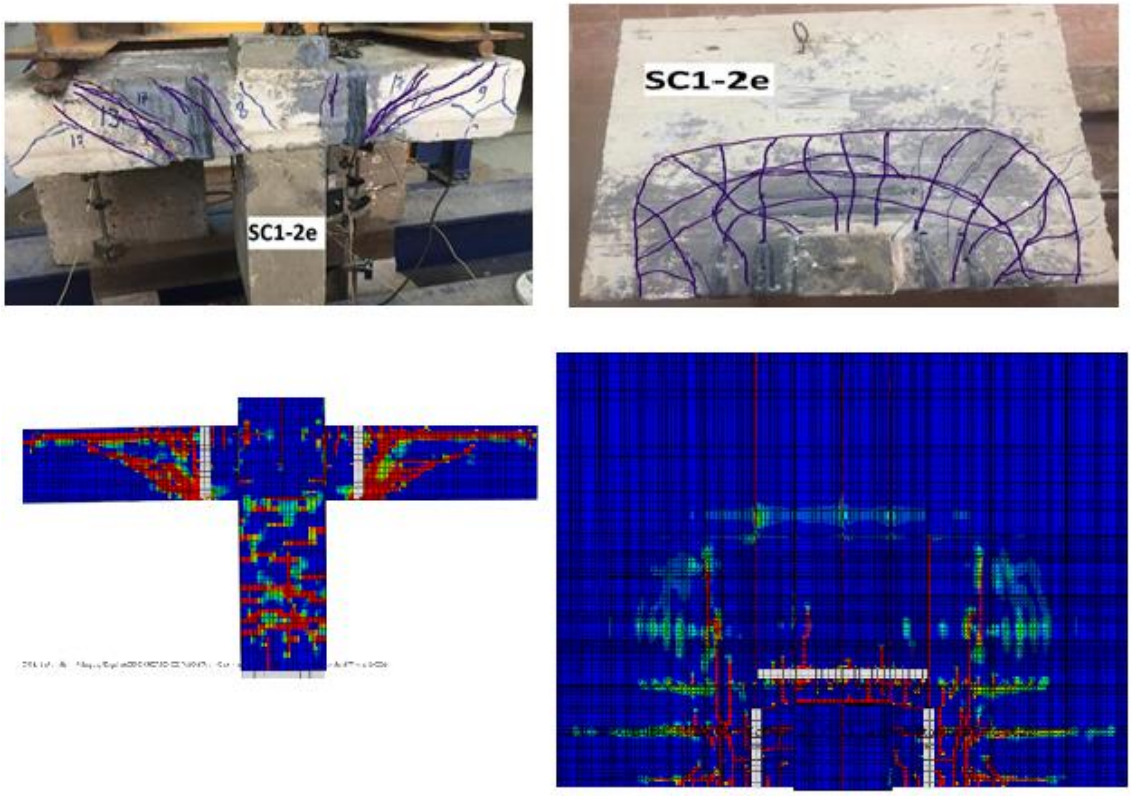

Fig. (38) FEM and Exp. pattern of failure comparison for specimen (SC1-2e).

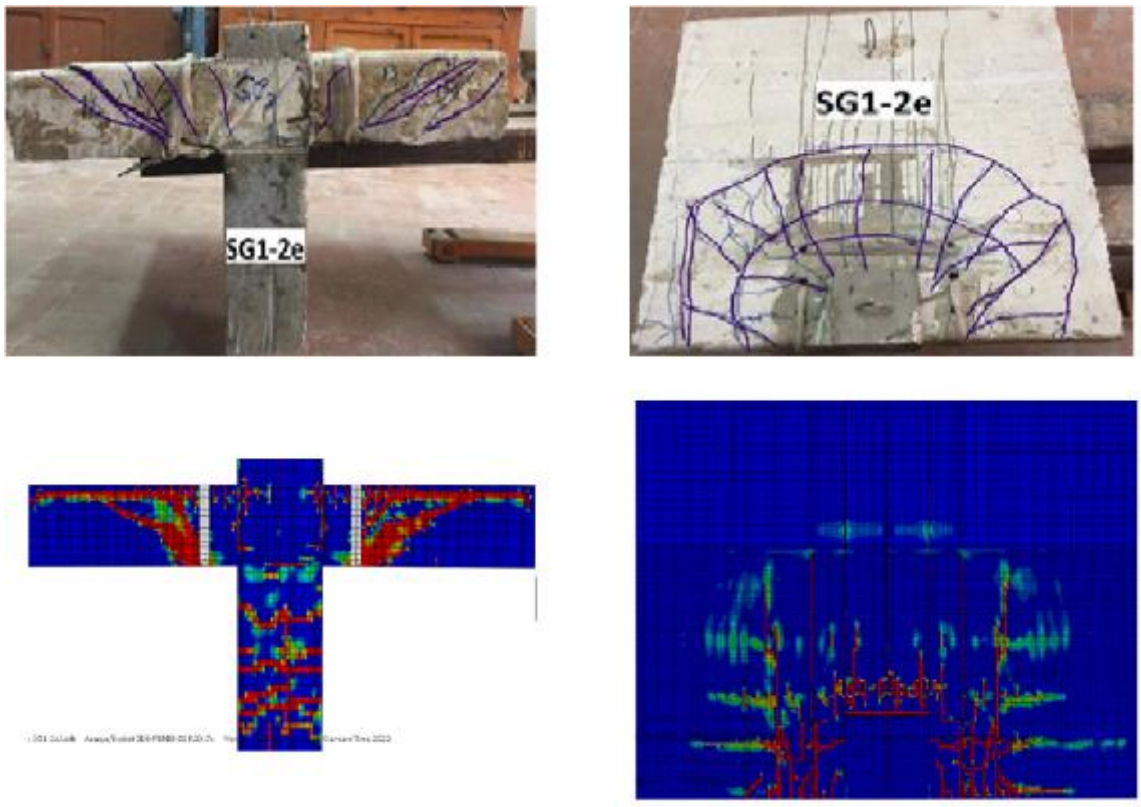

Fig. (39) FEM and Exp. pattern of failure comparison for specimen (SG1-2e).

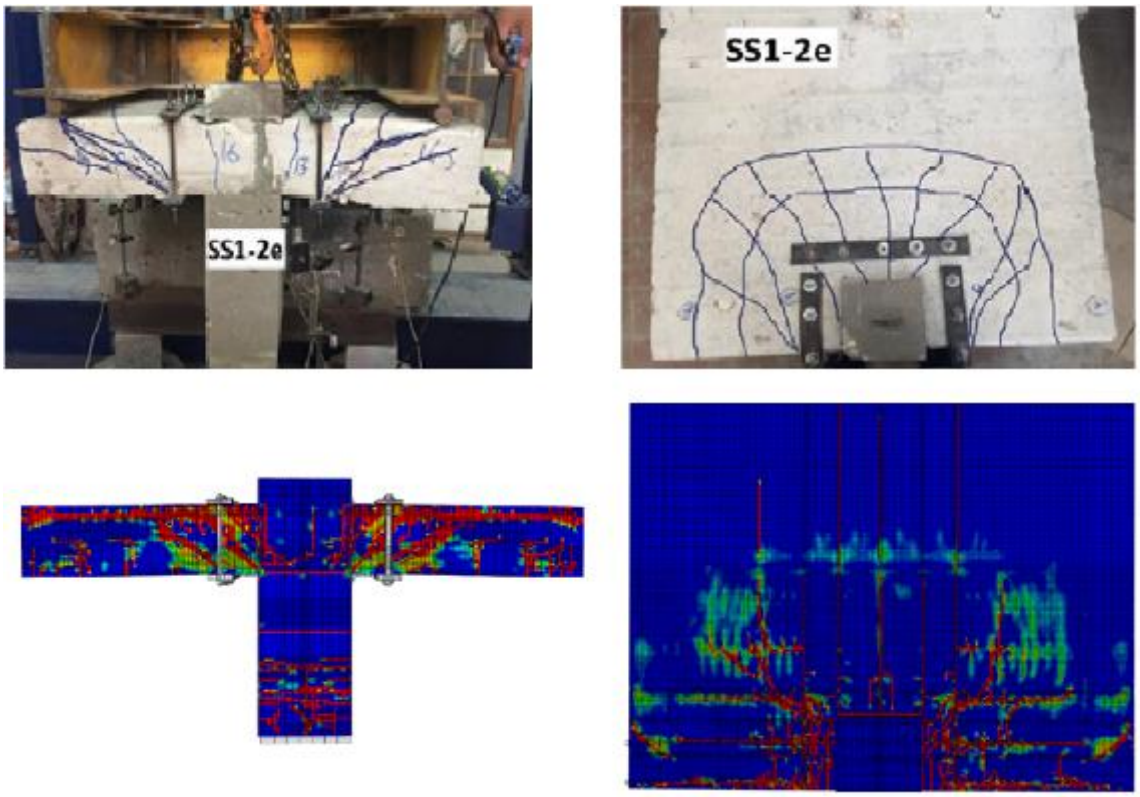

Fig. (40) FEM and Exp. pattern of failure comparison for specimen (SS1-2e).

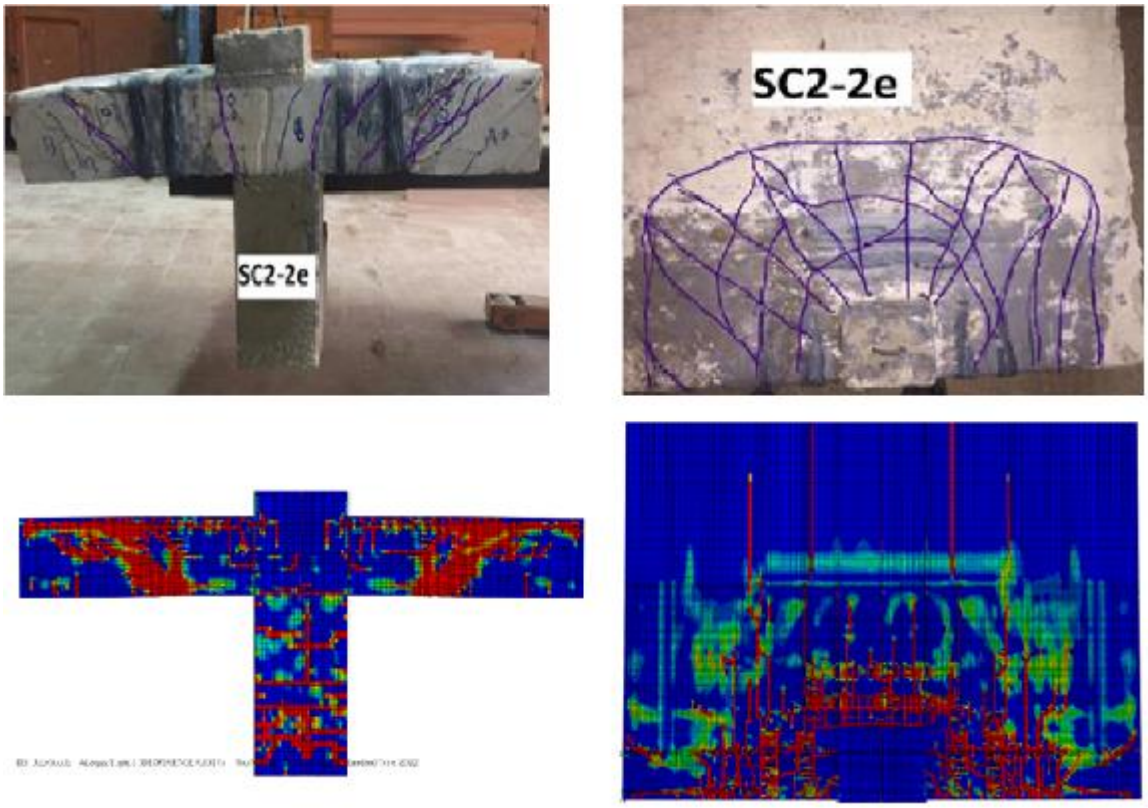

Fig. (41) FEM and Exp. pattern of failure comparison for specimen (SC2-2e).

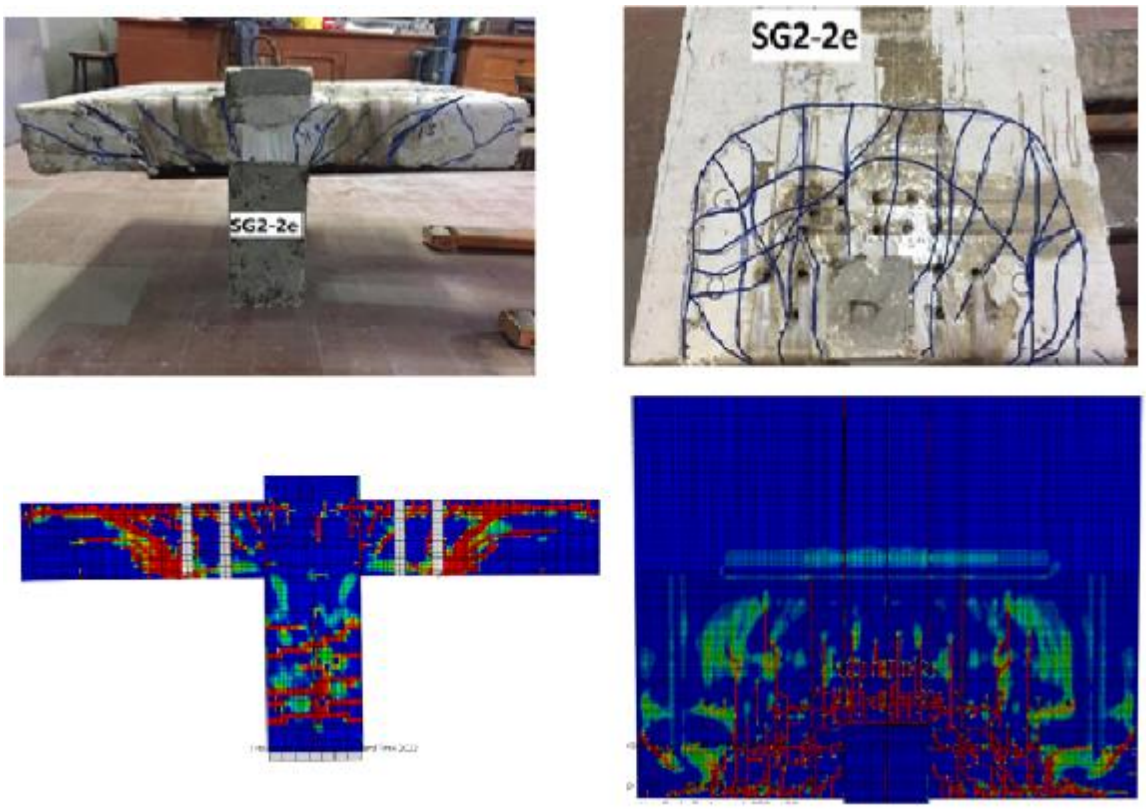

Fig. (42) FEM and Exp. pattern of failure comparison for specimen (SG2-2e).

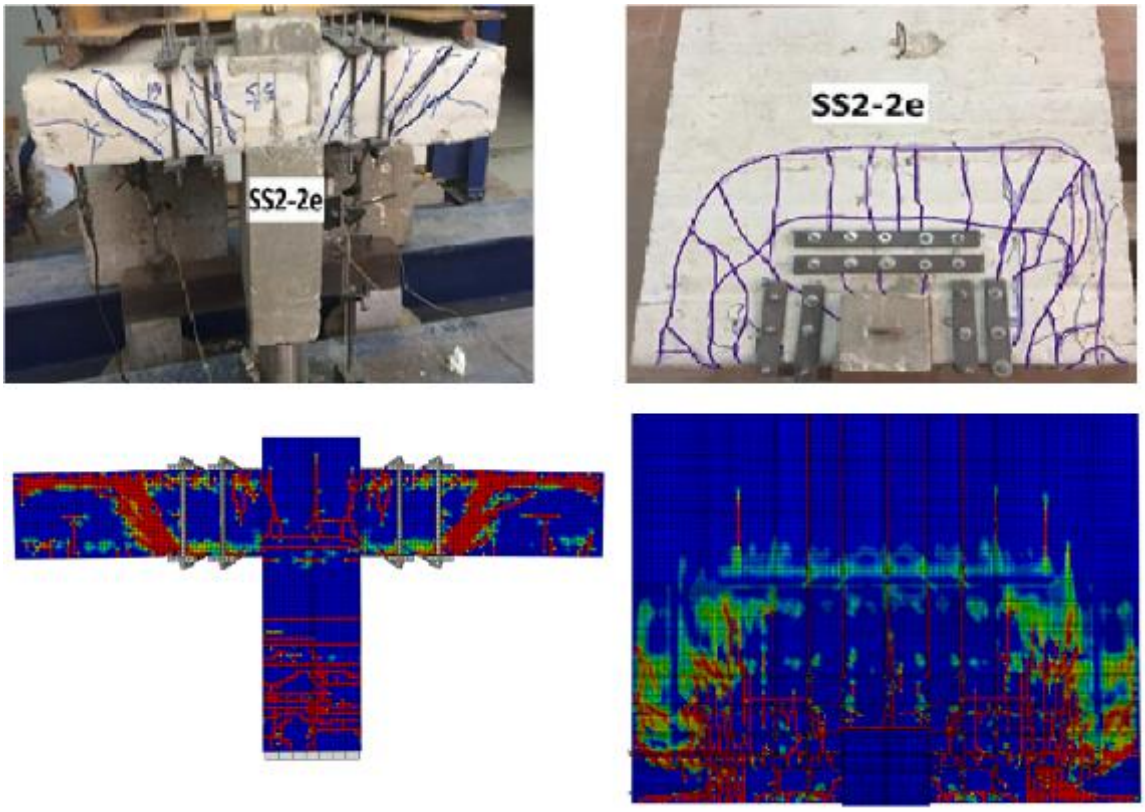

Fig. (43) FEM and Exp. pattern of failure comparison for specimen (SS2-2e).

4. Conclusions

1) Finite element modeling using ABAQUS software satisfactory simulates the structural behavior of flat slab edge column connections where excessive non-uniform shear stress is generated due to the eccentric acting load.
2) Similar to experimental specimens, all the FE specimens were failed due to punching shear stresses.
3) For all the FE specimens, the cracks initiated near the edges of the columns on the underside of the slab penetrating the slab to form an incomplete inverted cone, and the failure pattern was created entirely out of the strengthened zone.
4) Comparisons of load-deflection curves showed good agreement between all experimental sample results and the predicted FEM as a slight deviation was observed between the compared results.
5) The maximum difference between FEM and Experimental ultimate loads was 4.7% and the minimum difference was 0.6 %.
6) As experimental study concluded, FEM analysis showed that CFRP was the best effective material used for strengthening, as it gained the highest observed strength.
7) The good agreement between the numerical results and the corresponding experimental results confirms the validity of the parameters used to develop the proposed finite element model.
8) A future parametric study based on the proposed finite element model can be conducted to study the influence of various factors affecting the punching behavior of flat slab edge column connections.

5. References

[1] G. I. Khaleel, K. M. Elsayed and M. I. Omar, AN Experimental Study on Strengthening of R.C Flat Slab Edge Column Connections Subjected to Punching Shear Due to Eccentric Loads Using FRP, ENGINEERING JOURNAL Volume 2 Issue 2, DOI: 10.21608/MSAENG.2023.291871.

[2] A.S.Genikomsou, and M.A. Polak, Finite Element Analysis of a Reinforced Concrete Slab-Column Connection using ABAQUS, Structures Congress 2014 © ASCE 2014.

[3] P.E. Regan, M.W. Braestrup, Punching Shear in Reinforced Concrete—A State-of-the-Art Report; Bulletin d'Information No. 168; Comité Euro-International du Béton: Lausanne, Switzerland, 1985.

[4] Jia, Y, Chiang, J.C.L. Finite Element Analysis of Punching Shear of Reinforced Concrete Slab–Column Connections with Shear Reinforcement. Appl. Sci. 2022, 12, 9584.https://doi.org/10.3390/ app12199584.

[5] I Ketut Sudarsana 1 , I Gede Gegiranang Wiryadi 2, Finite element analysis of the effect M/V ratios on punching shear strength of edge slab column connections of flat plate structure, MATEC Web of Conferences 276, /doi.org/10.1051/matecconf /201927601012.

[6] N.J. Gardner, X.Y. Shao, ACI Struct. J. 93 (1996).

[7] I.K. Sudarsana, I.G. Wiryadi, I.G.A Susila, MATEC Web Conf. 159 (2018).

[8] G. J. Milligan, M. A. Polak, C. Zurell, Finite element analysis of punching shear behaviour of concrete slabs supported on rectangular columns, doi.org/10.1016/j.engstruct.2020.111189

[9] P. OS, Ferreira MP, O. DC, L. Neto AF, Teixeira MR. Influence of thecolumn rectangularity index and of the boundary conditions in the punching resistance of slab-column connections. Ibracon Struct Mater J 2015;8(3):260–95.

[10] A. S. Genikomsou, M. A. Polak, Finite element analysis of punching shear of concrete slabs using damaged plasticity model in ABAQUS, doi.org/10.1016/j.engstruct.2015.04.016.

[11] A. S. Genikomsou, S.M.ASCE ; and M. A. Polak, Finite-Element Analysis of Reinforced Concrete Slabs with Punching Shear Reinforcement M.ASCE2,DOI: 10.1061/(ASCE)ST.1943-541X.0001603.
© 2016 American Society of Civil Engineers.

[12] M. H. Makhlouf, G. I. Khalil, M. I. Badawi, Efficiency of (GFRP- Steel) Stirrups in Reinforcing the Punching of Slab-Column Connections subjected to Eccentric Load DOI: 10.21608/MSAENG.2023.291903.

[13] Y. Jia and J. Choong L. Chiang, Finite Element Analysis of Punching Shear of Reinforced Concrete Mushroom Slab-Column Connections Using ABAQUS, apply 2023Y. Yang (ed.), Advances in Frontier Research on Engineering Structures, Lecture Notes in Civil Engineering 286, https://doi.org/10.1007/978-981-19-8657-4_8

[14] L.F.A. Bernardo, and M.M. Teixeira, "Refined Softened-Truss Model with Efficient Solution Procedure for Reinforced Concrete Members under Torsion Combined with Bending", Structures 26, 2020, pp. 651–669.

[15] Kamal, M. M, Meleka, N. N., Tayel, M. A., and Mohamed R. M., "Repair and Strengthening of Flat Slabs Using Advanced Materials", Eleventh International Colloquium on Structural and Geotechnical Engineering, Ain Shams University, Faculty of Engineering, Department of Structural Engineering, 17-19 May 2005, pp. E05RC31-1-10.

[16] N. N. Meleka, M. A Tayel, and A. M. Ramadan, "Experimental Evaluation of Advanced Techniques for Repair and Strengthening of Reinforced Concrete Slabs", Alexandria Engineering Journal, Vol. 43, No. 3, May 2004.

[17] I. M. Othman, N. N. Meleka and Kh. M. Heiza, "Behavior of Reinforced Concrete Beams Strengthened by FRP Systems Subjected to Combined Bending and Torsion" Ph.D. thesis, Faculty of Engineering, Menoufia University, 2021.

[18] Abaqus Documentation User's Guide: ABAQUS User's Guide: Dassault Systemes, Simulia Corp, Providence, 2021.

19- Hu, Hsuam-Teh, and William C. Schnobrich. "Constitutive Modeling of Concrete by Using Nonassociated Plasticity." Journal of Materials in Civil Engineering 1, no. 4 (1989): 199-216.